

# Insights into surface-modified $\text{Li}(\text{Ni}_{0.80}\text{Co}_{0.15}\text{Al}_{0.05})\text{O}_2$ cathode by atomic layer fluorination for improved cycling behaviour

1

Youn Charles-Blin,<sup>a,b,e</sup> Oumaima Hatim,<sup>a</sup> Mélissa Clarac,<sup>a</sup> Anne-Marie Perbost,<sup>a</sup> Solveine Liminana,<sup>a</sup> Laura Lopez,<sup>a</sup> Olinda Gimello,<sup>a</sup> Katia Guérin,<sup>c</sup> Marc Dubois,<sup>c</sup> Michael Deschamps,<sup>d,e</sup> Delphine Flahaut,<sup>b,e</sup> Hervé Martinez,<sup>b,e</sup> Laure Monconduit,<sup>a,e</sup> and Nicolas Louvain\*<sup>a,e</sup>

- Institut Charles Gerhardt Montpellier, Université de Montpellier, CNRS, 34095 Montpellier, France.*
- CNRS/Univ. Pau & Pays Adour/E2S UPPA, Institut des Sciences Analytiques et de Physicochimie pour l'Environnement et les Matériaux - UMR 5254, 64000 Pau, France.*
- Université Clermont Auvergne, CNRS, Sigma Clermont, ICCF, 63000 Clermont-Ferrand, France.*
- CEMHTI, CNRS UPR 3079, Université d'Orléans, F45071 Orléans, France.*
- Réseau sur le Stockage Electrochimique de l'Energie (RS2E), FR CNRS 3459, 33 Rue Saint Leu, 80039 Amiens, France.*

\*email: nicolas.louvain@umontpellier.fr

## Methods

**Chemicals and materials.**  $\text{Li}(\text{Ni}_{0.80}\text{Co}_{0.15}\text{Al}_{0.05})\text{O}_2$ , NCA (NANOMYTE® BE-45, electrode micropowder, 11 - 13  $\mu\text{m}$  particle size, 50 - 70 nm grain size, > 98 % purity) was purchased from NEI Corporation. Xenon difluoride ( $\text{XeF}_2$ , 99.99 % trace metal basis), and lithium metal ribbon (Li, 99.9 % trace metal basis) were purchased from Sigma-Aldrich. Polytetrafluoroethylene PTFE 6N was obtained from DuPont™. Polyvinylidene fluoride PVDF (Solef® 5130/1001 PVDF, 1,1-difluoro-ethene, homopolymer, > 99.9 %) was purchased from Solvay. Carbon black Super C65 was purchased from Imerys Graphite & Carbon. GE Healthcare Life Sciences Whatman Grade GF/D glass microfiber filters (borosilicate;  $\varnothing$  55 mm, 675  $\mu\text{m}$  thickness) were purchased from Sigma-Aldrich.  $\text{LiPF}_6$  1 M in EC:DMC (1:1 vol.%) electrolyte (99.9 %,  $\text{H}_2\text{O} < 20$  ppm) was purchased from Solvionic. Except if explicitly noted, all syntheses, materials storage, sample preparation for characterization, and experiments have been carried out in an inert atmosphere and/or prepared in a glovebox ( $\text{H}_2\text{O} < 0.5$  ppm,  $\text{O}_2 < 0.5$  ppm).

**Synthesis of NCA-FX.** In a glovebox, NCA (300 mg, 3.12 mmol) was placed a thick-walled PTFE reactor vessel. Xenon difluoride (8 wt.% as compared to NCA; see Table S 1) was placed in a smaller PTFE container, and subsequently positioned in the reactor. The reactor was tightly closed, left undisturbed for 1h30 or 3h30 at room temperature, and finally opened.

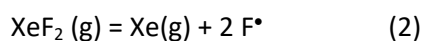
Table S 1. Synthesis parameters, and naming scheme.

	NCA	XeF <sub>2</sub>
wt.%	100	8
Mass (mg)	300	24
n (mmol)	3.12	0.14
n <sub>F</sub> (mmol)	--	0.28
1h30	--	NCA@F1
3h30	--	NCA@F2

Fluorinated NCA samples were prepared by fluorination through the controlled thermal decomposition of XeF<sub>2</sub>, using solid XeF<sub>2</sub>, thanks to the equilibrium:



Xenon difluoride has a vapor pressure of 3.8 mmHg at 25 °C, and 318 mmHg at 100 °C,<sup>1</sup> and is easily decomposed under heating, at the surface of a reactive material or UV irradiation,<sup>2</sup> according to the reaction:



The release of F<sup>•</sup> is constant and moderated because of the low saturating steam pressure of XeF<sub>2</sub>. While the fluorine content is usually obtained from weight uptake, it was almost impossible to determine accurately because of the static electricity leading to oxide particles sticking on PTFE surface.

**Solid state characterizations.** X-ray diffraction (XRD) experiments have been carried out on a PANalytical Empyrean diffractometer (Cu K $\alpha$  source) on powder samples. Fluorinated samples have been measured with a dedicated sample holder for air-sensitive materials covered with a Kapton foil from PANalytical, and prepared in glovebox (H<sub>2</sub>O < 0.5 ppm, O<sub>2</sub> < 0.5 ppm). Scanning electronic microscopy (SEM) was carried out on a Hitachi S4800 FE-SEM (voltage 5 kV). Energy dispersive X-ray spectrometry (EDX) was performed in a Zeiss EVO HD15 SEM instrument fitted with an Oxford Instruments X-Max<sup>N</sup> SDD EDX analyzer. The samples were prepared in a glovebox by placing powders on carbon tape (SEM), or carbon grid (TEM). Samples for SEM were metallized with carbon prior to the experiments.

**<sup>19</sup>F Nuclear magnetic resonance (NMR) measurements.** The <sup>19</sup>F NMR spectra were recorded on a 300 MHz Bruker spectrometer (Larmor frequency of 282.2 MHz for <sup>19</sup>F), equipped with a magic angle spinning (MAS) probehead using rotors of 2.5 mm outer diameter. The spinning rate was set to 25 and 30 kHz and the RF power was set to XXX kHz (resulting in a 90 ° pulse of 4.0  $\mu$ s at XX.X W of power). The baseline distortion free spectrum was recorded with a Hahn echo sequence (with 2x1 rotor periods echo time), with a recovery delay of 60 s to ensure the spectra were quantitative (i.e. > 5 T<sub>1</sub>) and 128 transients were recorded over an 800-ppm spectral width. The bearing, drive, and frame cooling gas was nitrogen to avoid any sample contamination. <sup>19</sup>F chemical shifts were externally referenced to trifluoroacetic acid CF<sub>3</sub>COOH and were referenced to trichlorofluoromethane CFCl<sub>3</sub> ( $\delta$ CF<sub>3</sub>COOH = -76.55 ppm vs  $\delta$ CFCl<sub>3</sub>). The spectra were fitted with DMFit.<sup>3</sup> In order to obtain quantitative data, PTFE was added to each sample and its NMR signal was used as an internal reference. By fitting the PTFE signal, and integrating it, it was possible to obtain quantitative data regarding the fluorinated samples.

**X-ray photoelectron spectroscopy (XPS) analysis.** Surface atomic composition and chemical environment of pristine and fluorinated materials were analysed by X-ray photoelectron spectroscopy

(XPS) technique on a Kratos Axis Ultra spectrometer with a hemispherical analyzer and a focused (analysis area is approximately  $200 \mu\text{m}^2$ ) monochromatized radiation Al K $\alpha$  line (1486.6 eV) operating at 75 W under a residual pressure of  $5 \times 10^{-9}$  mbar. The XPS spectrometer was directly connected to an argon dry glovebox to prevent the samples from moisture or air. The spectrometer pass energy was set to 160 eV and 20 eV for survey spectrum and core peak records, respectively. Surface charging was minimized using a neutralizer gun, which sprays the low energy electrons and Ar<sup>+</sup> ions over the sample surface. All the binding energies were calibrated at 285.0 eV for the C 1s component originating from the surface carbon contamination. The treatment of core peaks was carried out using a nonlinear Shirley-type background.<sup>4</sup> The peak positions and areas were optimized by a weighted least-squares fitting method using 70 % Gaussian and 30 % Lorentzian line shapes. The quantification of surface composition was based on Scofield's relative sensitivity factors.<sup>5</sup> All the XPS measurements were carried out several times at different points of the electrodes surfaces to prevent any reproducibility issue.

**Electrochemical measurements.** All measurements were performed at 25 °C on a BCS-805 battery cycler from BioLogic. Electrodes were prepared by mixing the active material (NCA, or fluorinated NCA; 80 wt.%), PVDF (6 wt.%), and Super C65 (14 wt.%) in an agate pestle. After several minutes of blending with a mortar, the mixture was transferred to an agate ball-milling jar (with four balls) and 1-Methyl-2-pyrrolidinone (purchased from Sigma-Aldrich, anhydrous, 99.5 %) was added. The mixture is then ball-milled softly at 500 rpm for 30 min. After the ball-milling step, the mixture was tape casted uniformly at  $150 \mu\text{m}$  onto an aluminum current collector (GoodFellow) using a 3540 bird film applicator from Elcometer, and subsequently dried at room temperature. The electrodes were cut with a disk puncher (12.7 mm diameter), and subsequently dried under dynamic vacuum for 12 h (3 h at 80 °C, and 9 h without heating) with a glass oven B-585 from Büchi. Two-electrode 316L stainless steel 2032 coin cells were assembled in a glovebox, using lithium disks ( $\varnothing$  1/8 inch, 3.18 mm) both as reference and counter-electrodes, glass fiber filters as separator, and LiPF<sub>6</sub> 1 M in EC:DMC as the electrolyte. Galvanostatic measurements were performed in the voltage range of 4.5-2.5 V vs Li<sup>+</sup>/Li at different current densities. The theoretical specific capacity C of NCA was considered equal to  $280.7 \text{ mA h g}^{-1}$ , for a 1-e<sup>-</sup> process. All current densities were calculated as C/n for a charge/discharge with n lithium ions (de)inserted in 1 h. The polarisation was calculated as the difference between the average charge and discharge voltage measured at half-charge/half-discharge capacity ( $E_{1/2}$ ).

**GC-MS conditions.** All analyses were performed using a gas chromatograph coupled to a mass spectrometer GCMS (Shimadzu QP2010 plus). The chromatographic separation was performed on a Supel-Q Plot capillary column (30 m x 0.32 i.d., 30  $\mu\text{m}$ ) from Supelco. The gas carrier was high purity helium at a constant flow of  $0.8 \text{ mL min}^{-1}$ . The temperature program was set to an initial temperature of 42 °C that was increased to a final temperature of 250 °C at a rate of  $10 \text{ °C min}^{-1}$ . The final temperature was kept for 5 min. The transfer line temperature was set to 250 °C. The injector was held at 300 °C and was used in split mode. Ionization was performed by EI at electron energy of 70 eV. Mass spectra were acquired in full scan mode (m/z 50-500). Compound identification and corresponding structural formula were assigned using the National Institutes of Standards (NIST) library.

Table S 2. Unit cells parameters obtained through profile matching, and final refinement factors.

	a (Å)	c (Å)	v (Å <sup>3</sup> )	R-factor	Rf-factor
<b>NCA 25°C</b>	2.865(1)	14.18(1)	100.86(7)	1.486	1.352
<b>NCA-F1 25°C</b>	2.865(8)	14.18(1)	100.85(8)	1.093	0.9515
<b>NCA-F2 25°C</b>	2.865(9)	14.18(3)	100.88(1)	0.695	0.7404

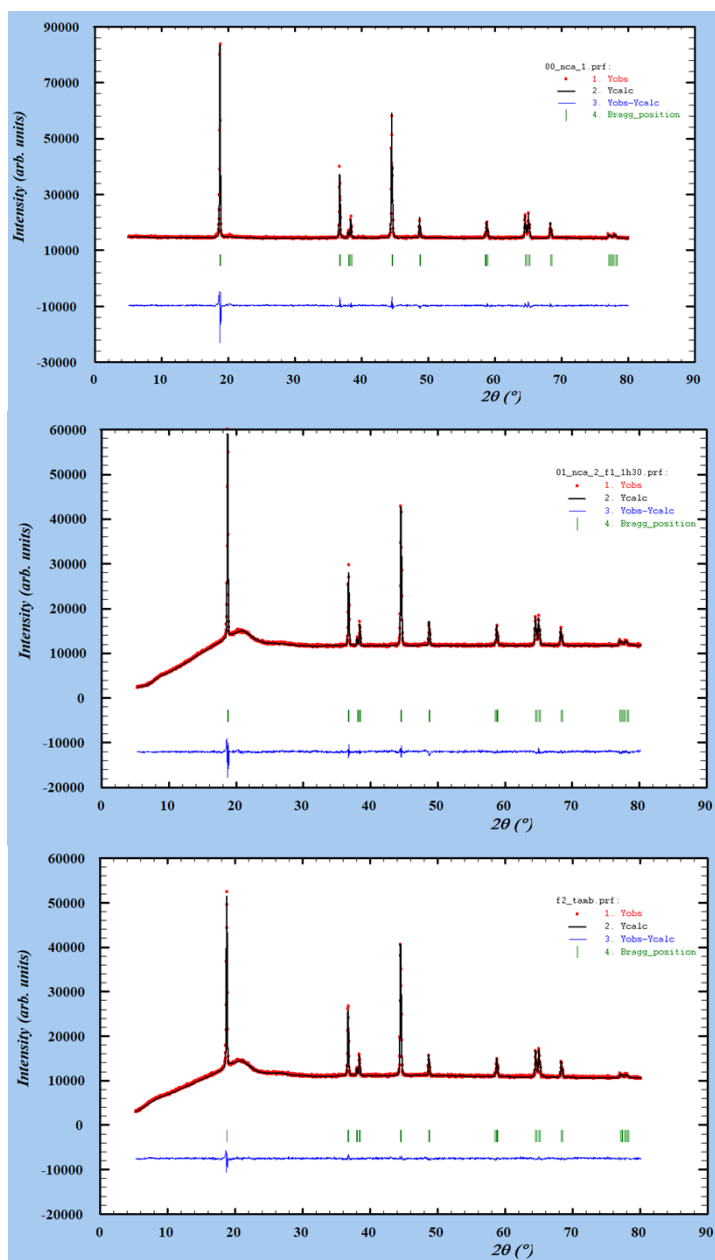
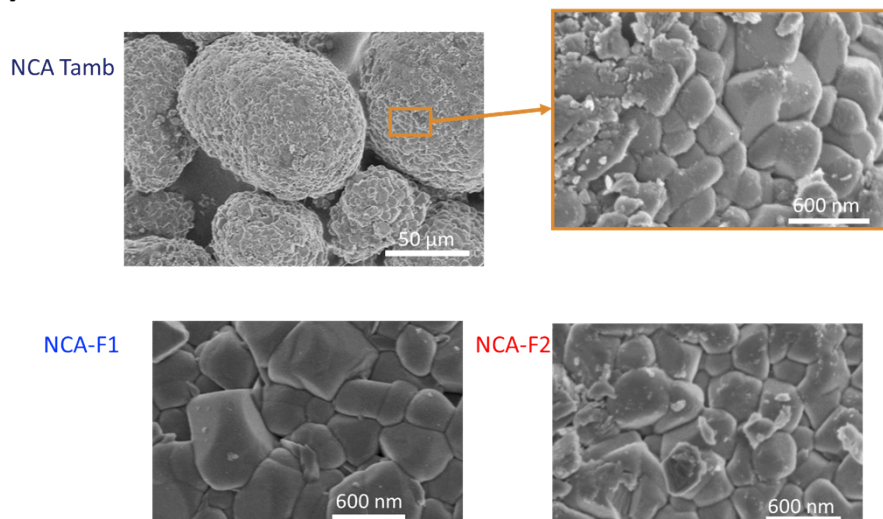


Figure S0. XRD Profile matching results of NCA, NCA-F1 and NCA-F2 samples.

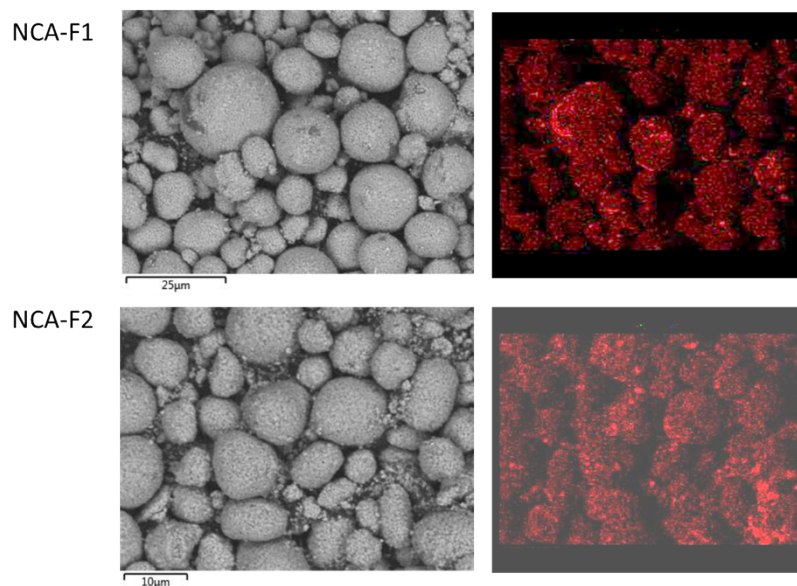
## SEM analysis



**Conclusion**  
= No morphology change  
= No clear difference after fluorination

Figure S 1. SEM images of NCA, NCA-F1 and NCA-F2 samples.

## EDX analysis



**Conclusion**  
= Fluorine detected  
= Fluorine repartition homogeneous

Figure S 2. EDX analysis of NCA-F1 and NCA-F2 samples.

Table S 3. Summary of F atom content (wt.%) extracted from  $^{19}\text{F}$  solid state NMR analysis.

## NMR analysis

### Expected from synthesis

Synthesis	NCA (mg)	XeF <sub>2</sub> (mg)	[F] (mg)	wt.% XeF <sub>2</sub>	mol.% XeF <sub>2</sub>	wt.% F	mol.% F	F (mmol)	Li <sub>1-2a</sub> (Ni <sub>0.80</sub> Co <sub>0.15</sub> Al <sub>0.05</sub> )O <sub>2</sub> + 2a LiF, 2a =
F1 = 8% XeF <sub>2</sub> 1h30 Room Temp	309,9	23,5	5,3	7,58%	4,30%	1,70%	8,60%	0,2776	0,09
F2 = 8% XeF <sub>2</sub> 3h30 Room temp	303,7	26,2	5,9	8,63%	4,89%	1,94%	9,79%	0,3095	0,1

### Results obtained from fitting NMR spectra

spinrate 30 kHz	NCA (mg)	PTFE (mg)	Itot% PTFE	Width PTFE (ppm)	Itot% F	Width F (ppm)	Itot%	wt.%F
F1 = 8% XeF <sub>2</sub> 1h30 Room temp	20,9	1,3	88,5%	3,09	11,4%	12,48	100%	0,8%
F2 = 8% XeF <sub>2</sub> 3h30 Room temp	21,0	1,4	82,5%	2,82	17,4%	13,36	100%	1,4%

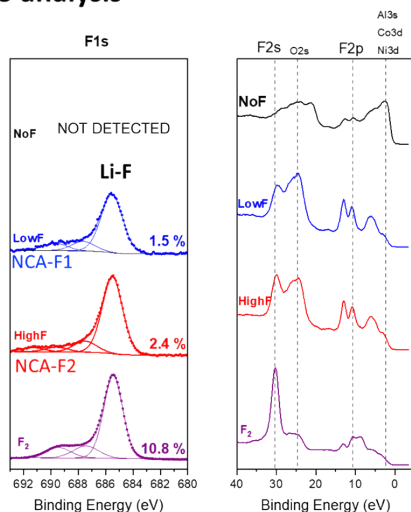
### Calculated from previous results

From NMR	NCA (mg)	XeF <sub>2</sub> (mg)	[F] (mg)	wt.% XeF <sub>2</sub>	mol.% XeF <sub>2</sub>	wt.% F	mol.% F	F (mmol)	Li <sub>1-2a</sub> (Ni <sub>0.80</sub> Co <sub>0.15</sub> Al <sub>0.05</sub> )O <sub>2</sub> + 2a LiF, 2a =	Yield (%)
F1 = 8% XeF <sub>2</sub> 1h30 Room Temp	309,9	(11,12)	2,495	3,59%	2,03%	0,8%	4,07%	0,1313	0,04	44%
F2 = 8% XeF <sub>2</sub> 3h30 Room temp	303,7	(19,07)	4,280	6,28%	3,56%	1,4%	7,12%	0,2253	0,07	70%

### Conclusion

- = Only a tiny amount of fluorine atoms!
- = Yield can still be improved.

## XPS analysis



### Results from XPS

= 1.5 at.% F for **NCA-F1**

$$F_{\text{Li-F}}/\text{Li}_{\text{Li-F}} = 0.26 \text{ (0.04 from NMR)}$$

= 2.4 at.% F for **NCA-F2**

$$F_{\text{Li-F}}/\text{Li}_{\text{Li-F}} = 0.38 \text{ (0.07 from NMR)}$$

To compare with  
NMR F% (coming from surface + bulk)

= we see valence band F = thickness over  
5 nm

Figure S 3. High resolution spectra of F 1s (left) and F 2s/2p (right) core peaks of reference and fluorinated pristine electrodes.

Table S 4. Binding energies (eV) and atomic percentages (at.%) of the surface environments of NCA, NCA-F1, and NCA-F2 powders.

Sample Iden Name	Position	%At Conc		Sample Iden Name	Position	%At Conc		Sample Iden Name	Position	%At Conc	
NCA_1_pt2	Al 2p	72.8	1.56	NCA_2_pt2	Al 2p	73.4	0.22	NCA_4_pt2	Al 2p	73.6	0.25
NOF pt2	Al 2p	73.2	0.78	LowF pt2	Al 2p	73.9	0.11	HighF pt2	Al 2p	74.0	0.13
			2.34				0.33				0.38
C 1s	C-C	285.0	21.78	C 1s	C-C	285.0	16.49	C 1s	C-C	285.0	20.97
C 1s	C-O	286.2	8.05	C 1s	C-O	286.0	7.05	C 1s	C-O	286.0	9.06
C 1s	Li2CO3	289.9	6.41	C 1s	Li2CO3	290.2	8.88	C 1s	Li2CO3	290.1	6.18
C 1s	*	291.9	0.38	C 1s		288.9	1.44	C 1s		289.1	2.57
C 1s	C=O	288.2	1.16	C 1s	CF2?	291.3	1.39	C 1s	CF2?	291.0	1.59
			37.78				35.25				40.37
Co 2p		797.1	0.01	Co 2p		796.5	0	Co 2p		790.5	0
Co 2p		807.1	0	Co 2p		780.4	0.02	Co 2p		780.3	0.02
Co 2p		779.8	0.15	Co 2p		795.5	0.01	Co 2p		796.1	0.01
Co 2p		794.9	0.08	Co 2p		792.7	0	Co 2p		795.2	0
Co 2p		789.9	0.01	Co 2p		790.7	0	Co 2p		781.6	0.01
Co 2p		786.6	0.02	Co 2p		782.3	0.03	Co 2p		783.5	0.01
Co 2p		804.2	0.01	Co 2p		788.2	0	Co 2p		772.7	0
Co 2p		780.9	0.09	Li 1s	Li2CO3	55.3	21.88	Li 1s	Li2CO3	55.4	19.84
Co 2p		783.8	0.06	Li 1s	NCA	54.3	0.63	Li 1s	NCA	54.4	0.61
			0.43	Li 1s	Li-F	56.5	4.22	Li 1s	Li-F	56.5	5.1
Li 1s	NCA	54.3	7.56				26.73				25.55
Li 1s	Li2CO3	55.4	11.85	Ni 2p		855.8	0.15	Ni 2p		855.8	0.17
			19.41	Ni 2p		873.2	0.05	Ni 2p		873.2	0.05
Ni 2p		855.2	1.16	Ni 2p		861.2	0.22	Ni 2p		861.1	0.3
Ni 2p		872.6	0.42	Ni 2p		879.5	0.09	Ni 2p		879.4	0.16
Ni 2p		861.5	0.83				0.51				0.68
Ni 2p		879.4	0.42	O 1s	oxide	529.7	0.63	O 1s	oxide	529.7	0.65
			2.83	O 1s	Li2CO3	532.0	27.43	O 1s	Li2CO3	532.0	22.75
O 1s	Oxide	529.3	7.31	O 1s	O-C	533.4	5.8	O 1s	O-C	533.3	4.74
O 1s	Li2CO3	531.8	23.04	O 1s		534.8	1.8	O 1s	CO3?	534.8	2.22
O 1s		533.6	5.27				35.66				30.36
O 1s		534.9	1.57	F 1s	Li-F	685.6	1.11	F 1s	Li-F	685.6	1.94
			37.19	F 1s	CF2/CF3?	689.7	0.15	F 1s	?	691.2	0.18
				F 1s	F inséré?	687.6	0.2	F 1s	inséré?	687.6	0.34
							1.46	F 1s	CF2? CF3?	689.7	0.15
											2.61

Report Copied on: Monday, October 22, 2018, 17:30:07

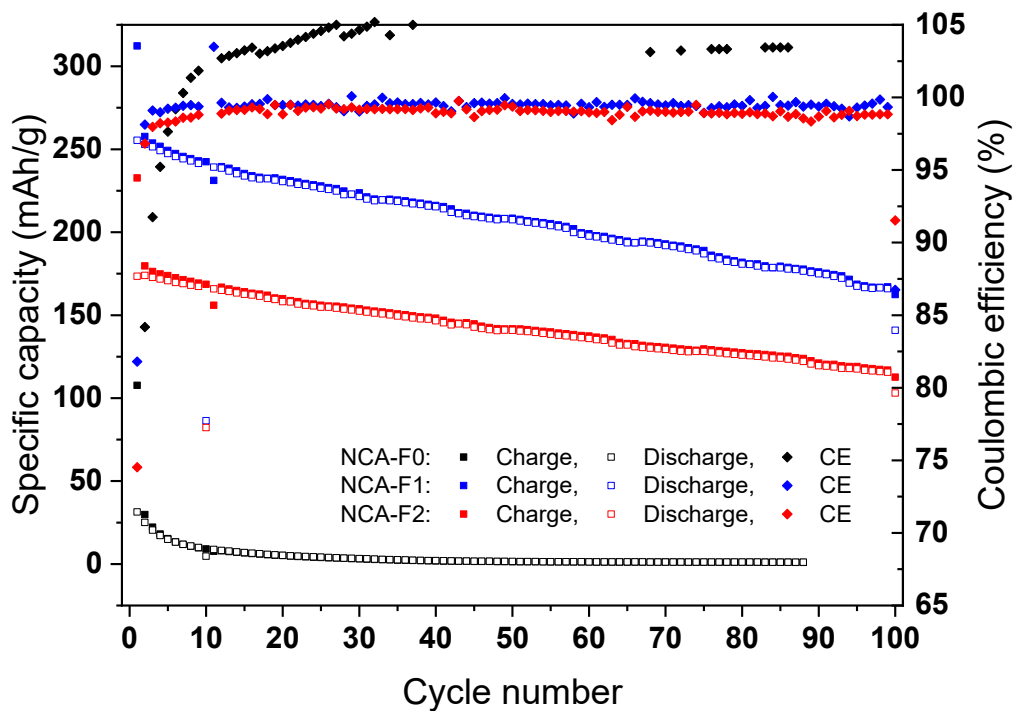


Figure S 4. Specific charge/discharge capacity and coulombic efficiency for NCA-F0/Li, NCA-F1/Li, and NCA-F2/Li cells cycled at C.

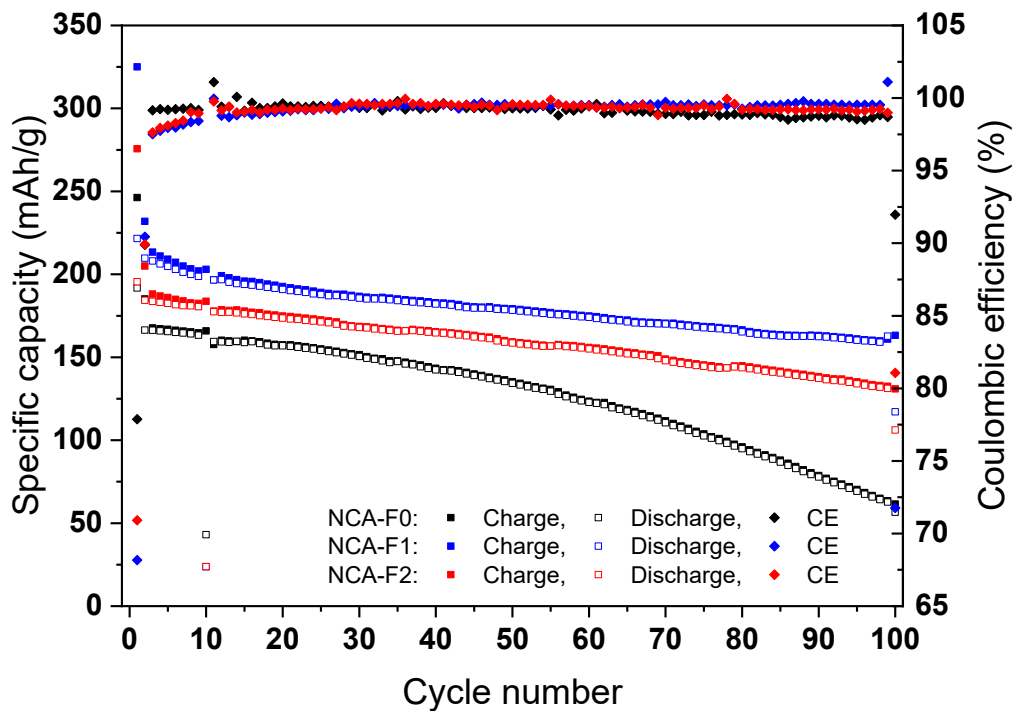
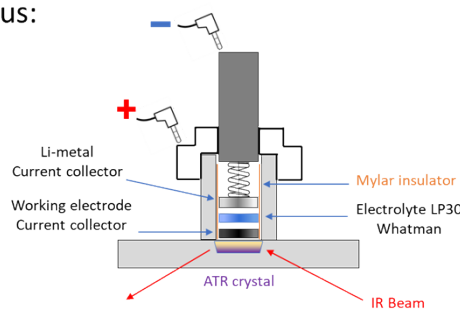


Figure S 5. Specific charge/discharge capacity and coulombic efficiency for NCA-F0/Li, NCA-F1/Li, and NCA-F2/Li cells cycled at C/5 for the first cycle, and subsequently at C.

# Operando ATR-FTIR

## • Experimental apparatus:



Annular electrode to study the electrolyte

Cell under Ar atmosphere  
Spectroscopy under synthetic air atmosphere

1<sup>st</sup> Background with the empty cell  
2<sup>nd</sup> Background ref electrode Li + whatmann+ electrolyte LP30

Acquisition duration= 30 s  
1 spectrum every 870 sec, 95 spectra IR per operando approximately

**Purpose :**  
Evaluate the influence of the fluorination at the interface in operando conditions

Figure S 6. Operando ATR-FTIR setup description.

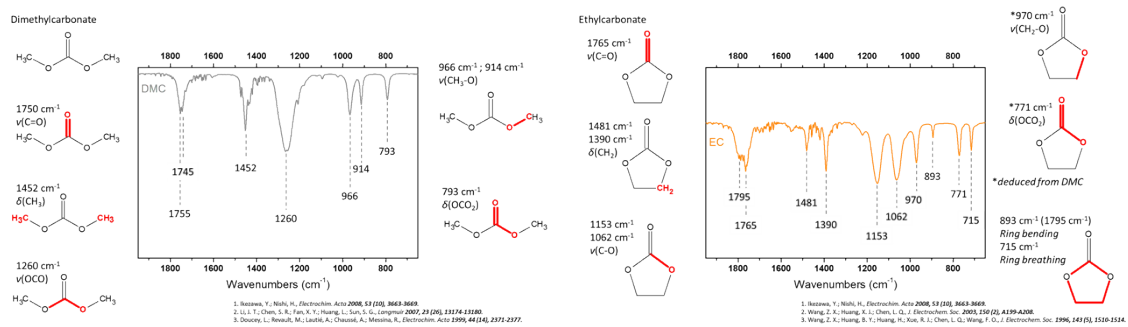


Figure S 7. FTIR spectra for dimethylcarbonate (left) and ethylene carbonate (right).

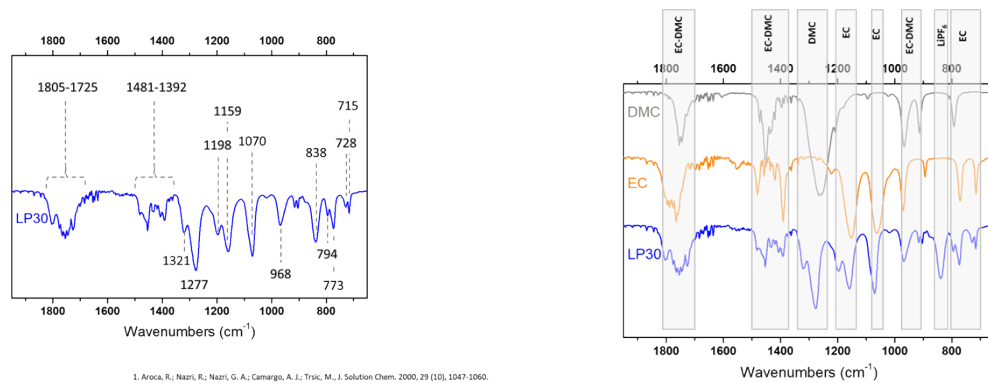


Figure S 8. FTIR spectra of LP30 (LiPF<sub>6</sub> 1 M in EC:DMC) electrolyte (left), and the comparison of LP30 with the solvents (right).

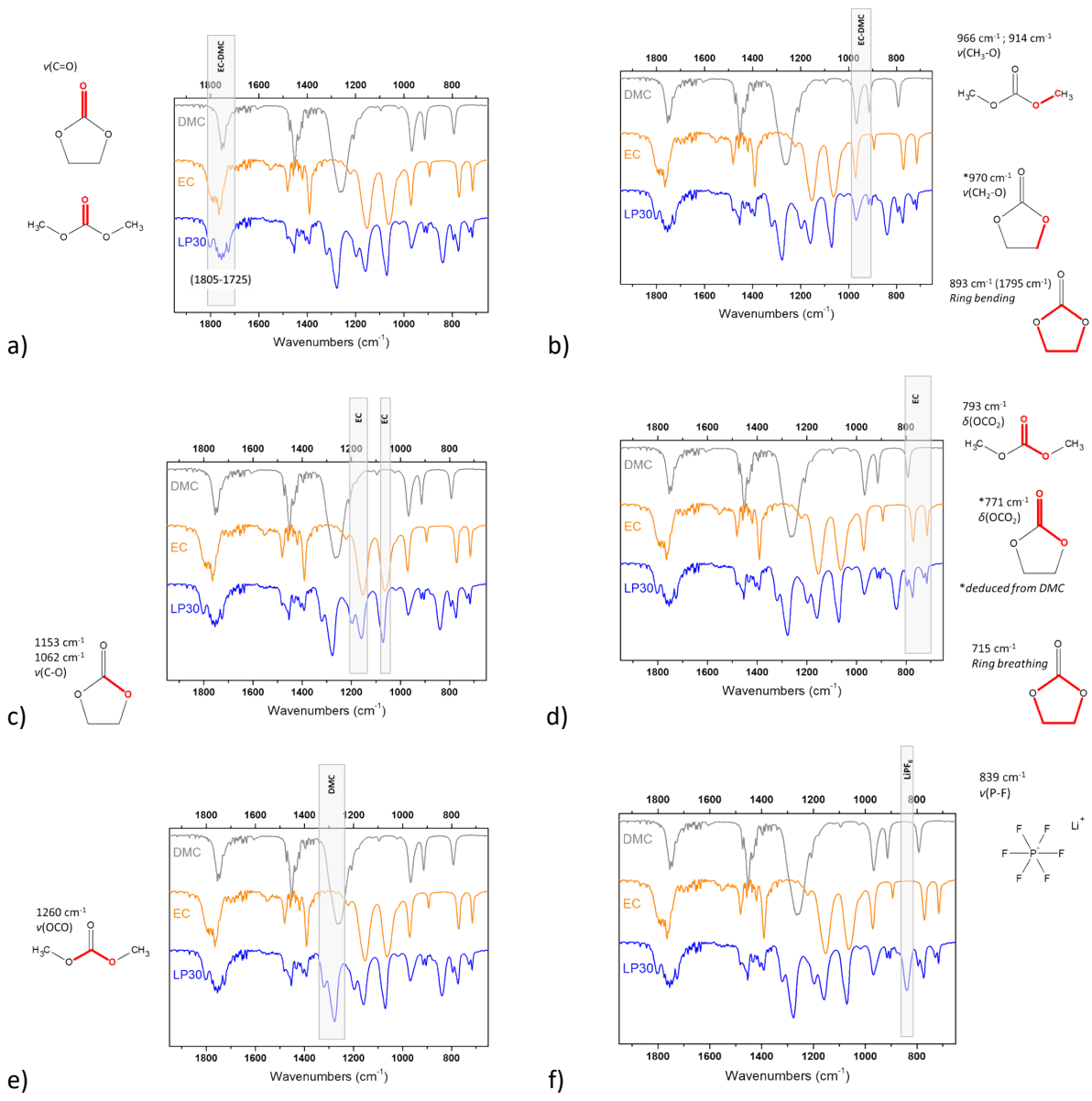


Figure S 9. FTIR spectra of EC, DMC, and LP30: emphasizing the contributions of each species to the FTIR signal; EC-DMC (a, b), EC (c, d), DMC (e), and LiPF<sub>6</sub> (f).

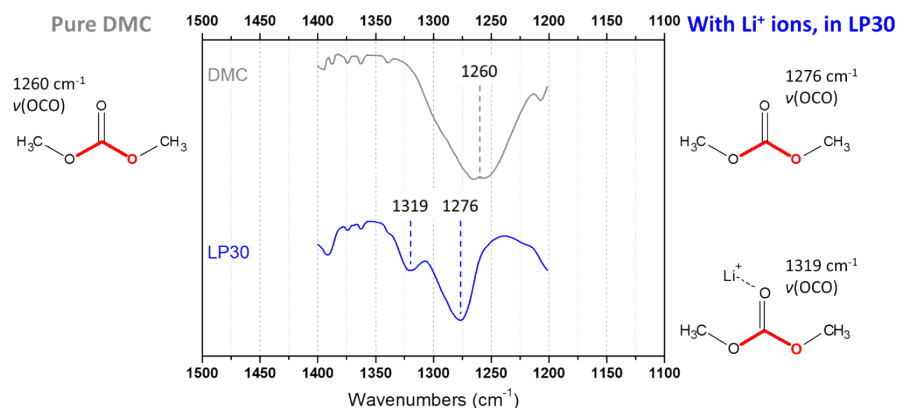


Figure S 10. Emphasizing the solvation of  $\text{Li}^+$  ions influence on the FTIR spectrum. Example of DMC and DMC-solvated lithium in LP30.

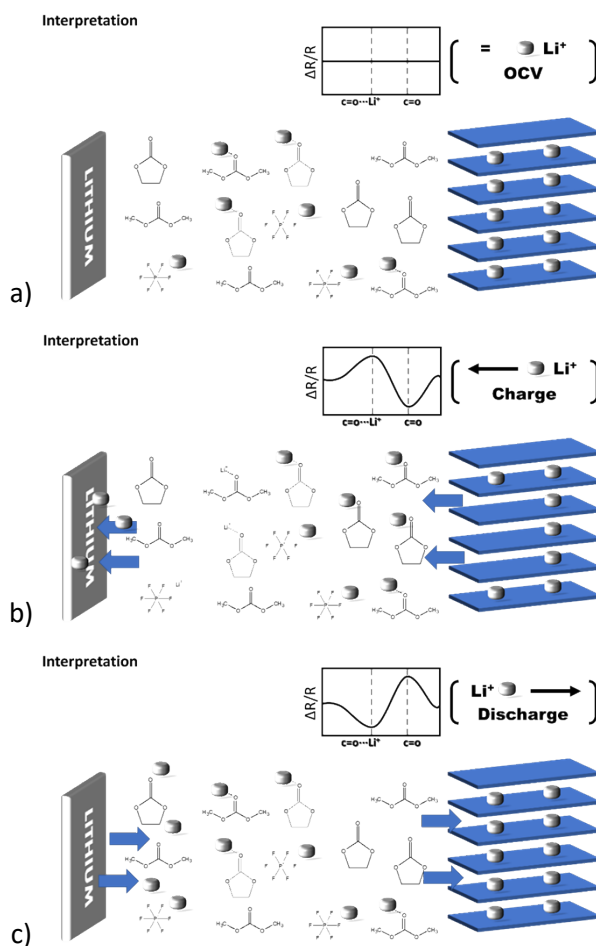


Figure S 11. Schematic illustration of the operando FTIR signal interpretation. A ratio of the selected spectrum, to which a reference spectrum is subtracted ( $\Delta R$ ), over the reference spectrum ( $\Delta R/R$ ) is used throughout the analysis for each material. The reference spectrum is the last recorded spectrum during the OCV, where the system is at equilibrium. The resulting  $\Delta R/R$  for the end of the OCV or the beginning of the cycling gives rise to a flat line (a). For the first charge, lithium ions are extracted from NCA, and the concentration of  $\text{Li}^+$  in the electrolyte will therefore increase at the vicinity of the cathode (where the diamond prism is located). The signal for solvated  $\text{Li}^+$  will thus increase (positive values) while the signal for solvents will go downward (b). During the discharge, or lithiation of the cathode, the behaviour is (or should be) reversible. Lithium ion concentration at cathode proximity will decrease, while the peak of the solvents will increase (c).

## Two GCPL cycles + ATR-FTIR

Procedure is  
the same for:  
NCA  
NCA-F1  
NCA-F2

●  
= FTIR  
measurement

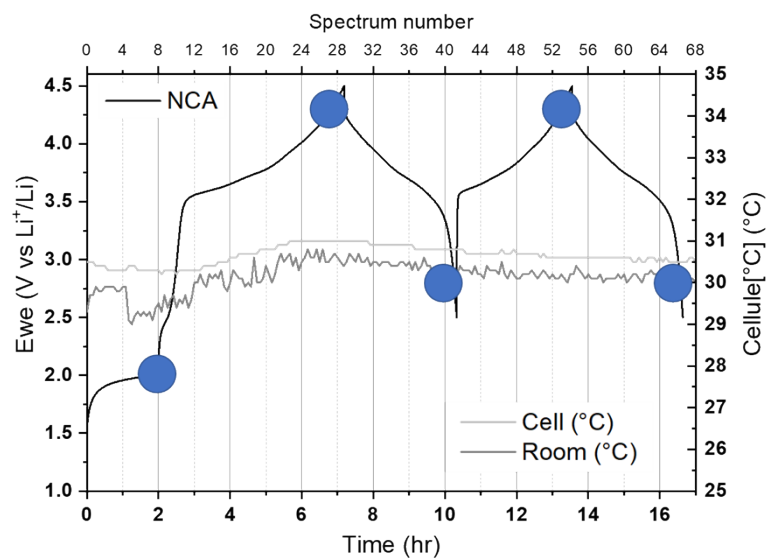


Figure S 12. Typical galvanostatic electrochemical measurement for operando ATR-FTIR measurement. Two galvanostatic cycles are investigated, and FTIR spectra are collected every 15 min. For the sake of clarity, some specific spectra are selected for comparison purpose, as indicated by the blue circles.

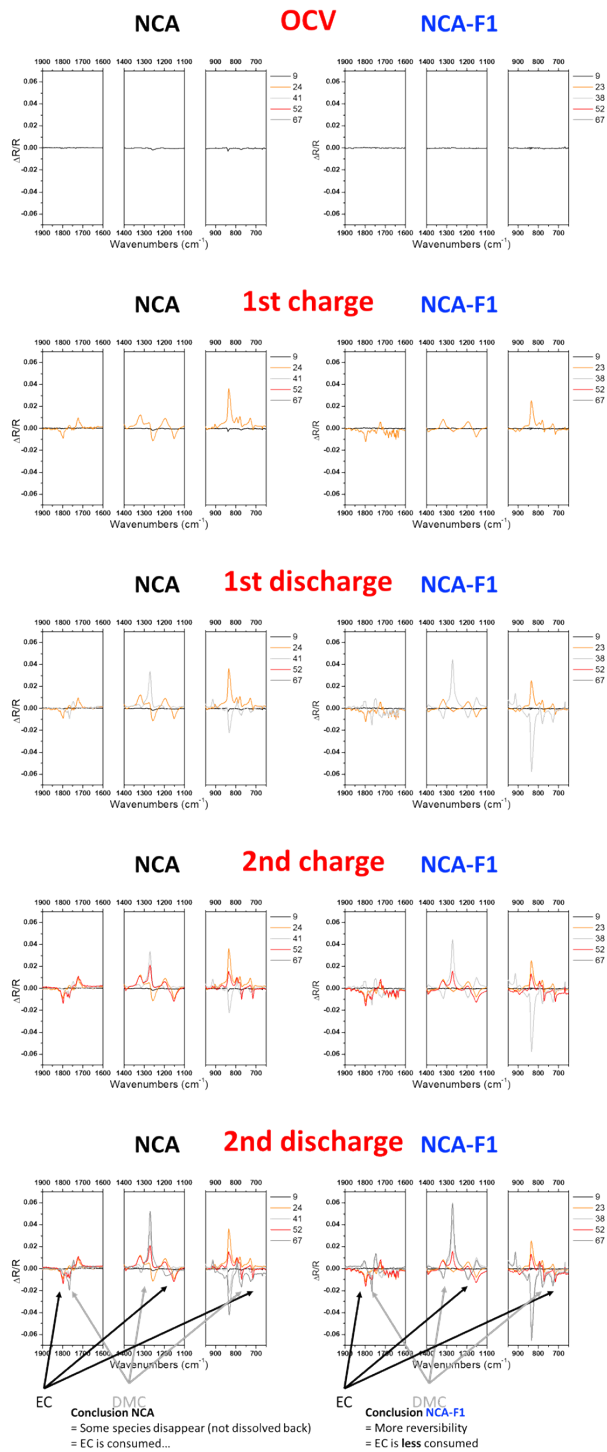


Figure S 13. Selected operando spectra for NCA vs Li and NCA-F1 vs Li half-cells.

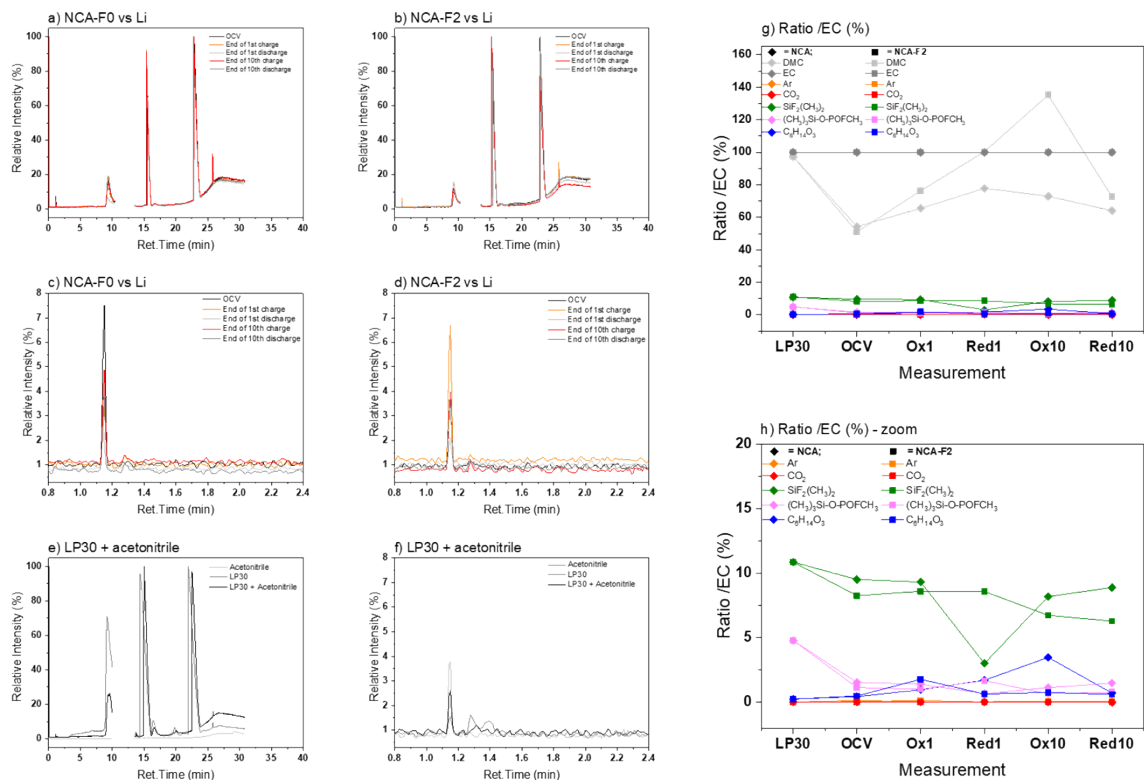


Figure S 14. GC-MS Chromatograms of electrolyte of NCA/Li half-cell (a) and NCA-F2/Li half-cell (b), and their corresponding zoom (c, d), measured post-mortem after 2 h of OCV, first charge, first discharge, 10<sup>th</sup> charge and 10<sup>th</sup> discharge, and of pristine LP30 electrolyte, acetonitrile, and a mix of both (e, f). Ratio of each contribution (area%) compared to EC (for all chromatograms, the relative abundance of the peak attributed to EC was always the highest and therefore normalized to 100 %) for LP30/acetonitrile, NCA, and NCA-F2 (g) and a zoom on the lower part (h).

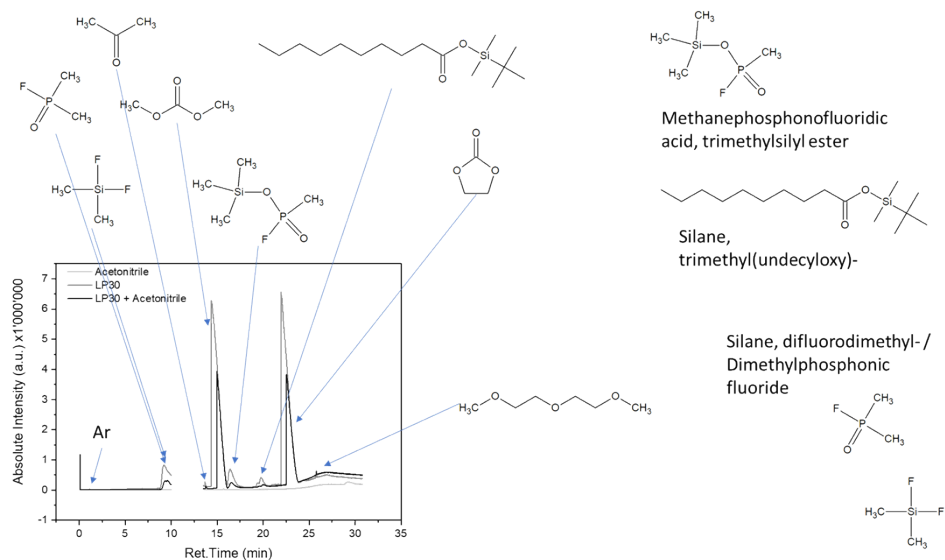


Figure S 15. Chromatograms of acetonitrile, LP30, and a mix LP30+acetonitrile, and the corresponding contributions as extracted from the GC-MS analysis (similarity search above 70%).

Table S 5. Summary of the GC-MS data for electrolytes of NCA-F0 (pristine NCA, not fluorinated), and NCA-F2, extracted from the GC-MS analysis: surface area (%) of each contribution in the chromatograms, and a ratio of each contribution considering EC as the main species. The last table, below, is related to the analysis of pristine LP30 electrolyte mixed with acetonitrile.

		Ar	CO2	SiF2Me2	Unknown	DMC	Me3-O-PFON	EC	Ether
NCA-F0 (Area%)	OCV	0.09	0.02	5.73	0.24	32.65	0.93	60.07	0.27
	Ox1	0.03	0.01	5.25	0.22	36.84	0.80	56.29	0.55
	Red1	0.03	0.01	1.65	0.07	42.43	0.37	54.51	0.94
	Ox10	0.04	0.01	4.41	0.09	39.21	0.61	53.75	1.88
	Red10	0.04	0.00	5.07	0.13	36.49	0.85	57.00	0.42
NCA-F0 Ratio /EC (%)	OCV	0.15	0.03	9.53	0.40	54.35	1.54	100.00	0.45
	Ox1	0.05	0.03	9.33	0.39	65.45	1.42	100.00	0.99
	Red1	0.05	0.01	3.02	0.13	77.83	0.68	100.00	1.72
	Ox10	0.08	0.01	8.20	0.18	72.96	1.14	100.00	3.49
	Red10	0.06	0.01	8.90	0.22	64.03	1.50	100.00	0.73
NCA-F2 (Area%)	OCV	0.04	0.01	5.13	0.13	31.65	0.72	62.01	0.31
	Ox1	0.08	0.00	4.58	0.09	40.56	0.54	53.19	0.96
	Red1	0.02	0.00	4.06	0.11	47.45	0.79	47.26	0.31
	Ox10	0.03	0.00	2.77	-0.02	55.54	0.28	41.07	0.32
	Red10	0.04	0.01	3.49	0.04	40.22	0.44	55.41	0.34
NCA-F2 Ratio /EC (%)	OCV	0.07	0.01	8.27	0.21	51.03	1.15	100.00	0.50
	Ox1	0.15	0.00	8.61	0.17	76.25	1.02	100.00	1.80
	Red1	0.04	0.01	8.60	0.24	100.40	1.68	100.00	0.65
	Ox10	0.08	0.01	6.75	-0.05	135.23	0.68	100.00	0.78
	Red10	0.07	0.01	6.30	0.07	72.59	0.80	100.00	0.62

		Ar	CO2	SiF2Me2	Acetone	DMC	Me3-O-PFON	Silane	EC	Ether
LP30+ACN	/DMC	0.02	0.01	11.18	0.53	100.00	4.94	1.81	102.81	0.27
	/EC	0.02	0.01	10.88	0.51	97.27	4.81	1.76	100.00	0.26

## References

1. J. G. Malm, H. Selig, J. Jortner and S. A. Rice, *Chem. Rev.*, 1965, **65**, 199-236.
2. E. Unger, M. Liebau, G. S. Duesberg, A. P. Graham, F. Kreupl, R. Seidel and W. Hoenlein, *Chem. Phys. Lett.*, 2004, **399**, 280-283.
3. D. Massiot, F. Fayon, M. Capron, I. King, S. Le Calve, B. Alonso, J. O. Durand, B. Bujoli, Z. H. Gan and G. Hoatson, *Magn. Reson. Chem.*, 2002, **40**, 70-76.
4. D. A. Shirley, *Phys Rev B*, 1972, **5**, 4709-4714.
5. J. H. Scofield, *J. Electron. Spectrosc. Relat. Phenom.*, 1976, **8**, 129-137.